Article

# Synthesis of SnS/SnS Fullerene-like Nanoparticles: A Superlattice with Polyhedral Shape

Sung You Hong, Ronit Popovitz-Biro, Yehiam Prior, and Reshef Tenne

*J. Am. Chem. Soc.*, **2003**, 125 (34), 10470-10474• DOI: 10.1021/ja036057d • Publication Date (Web): 31 July 2003



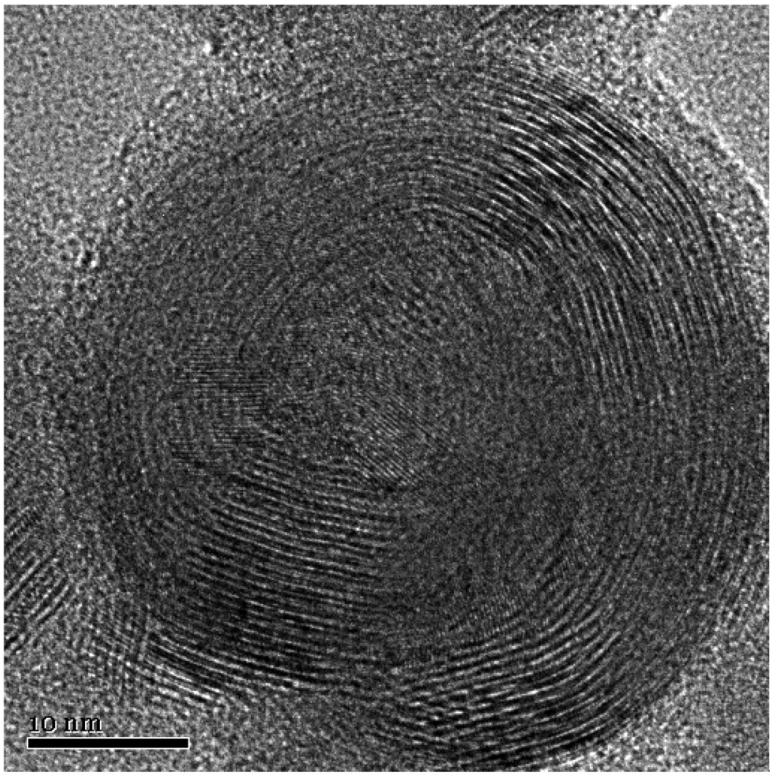


## More About This Article

Additional resources and features associated with this article are available within the HTML version:

- Supporting Information
- Links to the 6 articles that cite this article, as of the time of this article download
- Access to high resolution figures
- Links to articles and content related to this article
- Copyright permission to reproduce figures and/or text from this article

J|A|C|S
ARTICLES
Published on Web 07/31/2003

# Synthesis of $SnS_2$/SnS Fullerene-like Nanoparticles: A Superlattice with Polyhedral Shape

Sung You Hong,[†,§] Ronit Popovitz-Biro,*[,†] Yehiam Prior,[‡] and Reshef Tenne*[,†]

*Contribution from the Department of Materials and Interfaces and Department of Chemical Physics, Weizmann Institute of Science, Rehovot 76100, Israel, and School of Chemical Engineering, Seoul National University, Seoul 151-742, Korea*

Received May 10, 2003; E-mail: ronit.popovitz@weizmann.ac.il; reshef.tenne@weizmann.ac.il

***Abstract:*** Tin disulfide pellets were laser ablated in an inert gas atmosphere, and closed cage fullerene-like (*IF*) nanoparticles were produced. The nanoparticles had various polyhedra and short tubular structures. Some of these forms contained a periodic pattern of fringes resulting in a superstructure. These patterns could be assigned to a superlattice created by periodic stacking of layered $SnS_2$ and SnS. Such superlattices are reminiscent of misfit layer compounds, which are known to form tubular morphologies. This mechanism adds up to the established mechanism for *IF* formation, namely, the annihilation of reactive dangling bonds at the periphery of the nanoparticles. Additionally, it suggests that one of the driving forces to form tubules in misfit compounds is the annihilation of dangling bonds at the rim of the layered structure.

## 1. Introduction

Nanoparticles of inorganic layered compounds, like $MoS_2$, are known to form closed cage structures. Folding and bonding of edge atoms on the periphery of the quasi two-dimensional planar nanostructure lead to the formation of closed cages with polyhedral or nanotubular shapes.[1−3] Previously, nano-octahedra of $MoS_2$,[4] nanotubes, and closed cage fullerene-like structures of $NiCl_2$,[5] $WS_2$, and $MoS_2$[6] were produced by laser ablation. In the present work, laser ablation of a $SnS_2$ powder is carried out under a controlled atmosphere. This process leads to the formation of nanoparticles with polyhedral and short tubular shapes.

Tin disulfide is an inorganic compound, which crystallizes in the $PbI_2$ layered structure with a hexagonal primitive unit cell, in which the tin atoms are located in octahedral interstices between two hexagonally close packed sulfur slabs to form a three-atom layered sandwich structure.[7,8] More than 70 polytype structures of $SnS_2$ have been established. The polytypism arises from the different stacking of the 2-D molecular layers.[9−11] The thermodynamically stable polytype of $SnS_2$ at ambient conditions consists of a trigonal lattice $P3m$ ($a = 0.36486$ nm; $c = 0.58992$ nm) with one layer as a repeat unit. Among the tin−sulfur series of compounds, the SnS (Herzenbergite) is also known.[12] This material has a GeS structure with an orthorhombic unit cell $Pnma$ ($a = 1.118$ nm; $b = 0.398$ nm; $c = 0.432$ nm). Each tin atom is coordinated to six sulfur atoms in a highly distorted octahedral geometry. There are two corrugated tin−sulfide double layers in a unit cell.

## 2. Experimental Section

$SnS_2$ powder (Alfa Aesar, 99.5% pure) was pressed into a pellet (diameter: 17 mm). The target was put inside a quartz tube reactor heated to 150 °C. Laser ablation was conducted using a mildly focused pulsed, frequency-doubled Nd:YAG laser (532 nm, 50 Hz, 8 ns, 25−50 mJ (1.8−3.7 J $cm^{-2}$) per pulse) for 5 min. The focused spot was scanned continually across the pellet surface. The generated soot was flushed back downstream by the flowing argon gas and was collected on a quartz substrate, which was placed on a water-cooled finger outside the oven. The flow rate was set to 210 $cm^3$ $min^{-1}$, and the pressure was 760 Torr.

The collected powder was sonicated in ethanol, placed on a carbon/collodion-coated Cu grid, and analyzed by transmission electron microscopy (TEM, Philips CM-120, 120 kV), high-resolution transmission electron microscopy (HRTEM, FEI Tecnai F-30, 300 kV), and energy-dispersive X-ray spectroscopy (EDS, EDAX Phoenix). X-ray diffraction (XRD) was carried out with a Rigaku model D/MAX-B XRD equipped with a graphite-monochromatized Cu Kα radiation (1.54178 Å) anode. Raman measurements were carried out with a Renishaw model 1000 MicroRaman microscope equipped with a 25 mW He−Ne 632.8 nm laser.

† Department of Materials and Interfaces, Weizmann Institute of Science.
‡ Department of Chemical Physics, Weizmann Institute of Science.
§ Seoul National University.

(1) Tenne, R. *Chem. Eur. J.* **2002**, *8*, 5296.
(2) Tenne, R.; Margulis, L.; Genut, M.; Hodes, G. *Nature* **1992**, *360*, 444.
(3) Margulis, L.; Salitra, G.; Tenne, R.; Talianker, M. *Nature* **1993**, *365*, 113.
(4) Parilla, P. A.; Dillon, A. C.; Jones, K. M.; Riker, G.; Schulz, D. L.; Ginley, D. S.; Heben, M. J. *Nature* **1999**, *397*, 114.
(5) Rosenfeld Hacohen, Y.; Popovitz-Biro, R.; Grunbaum, E.; Prior, Y.; Tenne, R. *Adv. Mater.* **2002**, *14*, 1075.
(6) Sen, R.; Govindaraj, A.; Suenaga, K.; Suzuki, S.; Kataura, H.; Iijima, S.; Achiba, Y. *Chem. Phys. Lett.* **2001**, *340*, 242.
(7) Fong, C. Y.; Cohen, M. L. *Phys. Rev. B* **1972**, *5*, 3095.
(8) Domingo, G.; Itoga, R. S.; Kannewurf, C. R. *Phys. Rev.* **1966**, *143*, 536.
(9) Jiang, T.; Ozin, G. A. *J. Mater. Chem.* **1998**, *8*, 1099.
(10) Al-Alamy, F. A. S.; Balchin, A. A.; White, M. *J. Mater. Sci.* **1977**, *12*, 2037.
(11) Palosz, B.; W. Steurer; Schulz, H. *Acta Crystallogr.* **1990**, *B46*, 449.
(12) Jiang T.; Ozin, G. A. *J. Mater. Chem.* **1998**, *8*, 1099.


**10.1021/ja036057d CCC: $25.00** 

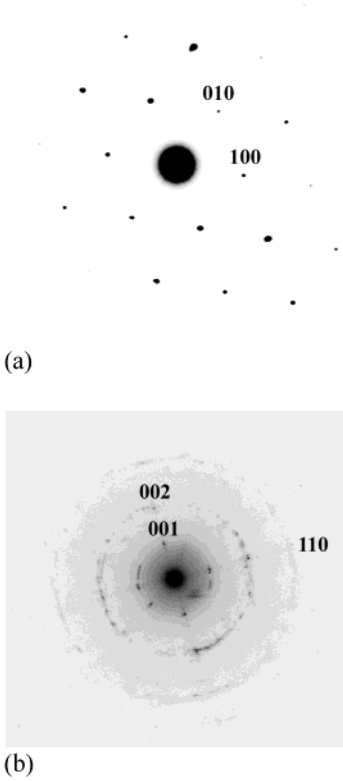


***Figure 1.*** Selected area electron diffraction pattern of (a) $SnS_2$ platelet, viewed along the [001] direction, and (b) $SnS_2$ polyhedra.

## 3. Results and Discussion

The analyzed soot included polyhedra and short nanotubes as well as platelets and nonlayered amorphous spherical nanodots. The energy per pulse (25−50 mJ per pulse) of the laser beam was varied during a series of experiments. However, no clear correlation between the ratio of polyhedral and nanotubular structures with the pulse energy was observed. To analyze the crystal structure of particles in the soot, XRD analyses were carried out. All the diffraction peaks of the as-prepared powder could be readily indexed to the 2T-$SnS_2$ (JCPDS card No. 23-0677). Raman analysis of the soot did not show any appreciable difference from the bulk sample, with main lines appearing at 314, 575/603, 827, and 1648 $cm^{-1}$.

Figure 1a displays selected area electron diffraction (SAED) of a single platelet, from bulk 2T-$SnS_2$, exhibiting a clear trigonal pattern. On the other hand, the SAED pattern (Figure 1b) of the *IF*-$SnS_2$ nanoparticles appears as a ring pattern. The calculated *d* spacings between two adjacent layers is 0.59 nm, in agreement with bulk $SnS_2$.

TEM imaging reveals that polyhedra of various forms, some with round and others with faceted morphology, were obtained (Figure 2). Both forms of polyhedra were in fact nested structures, i.e., closed multilayer nanostructures. The number of layers was usually larger than 10. Varying the tilt angle of the sample in the TEM, it was found that some parts of the fringe pattern of the polyhedron disappeared, while a different fringe pattern appeared on the other side of the nanostructure. This behavior was previously observed for closed cage nanoparticles of other layered compounds, like $CdCl_2$.[13] It could

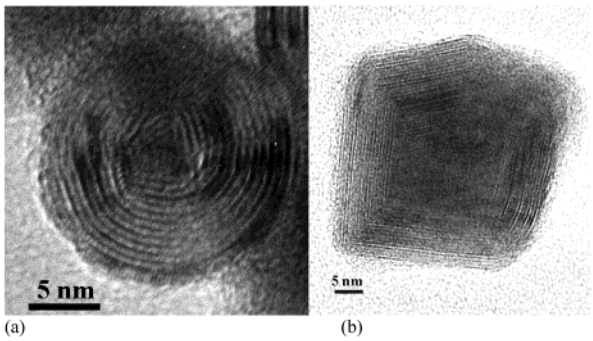


***Figure 2.*** TEM images of nanoparticles of (a) round type and (b) faceted type polyhedra.

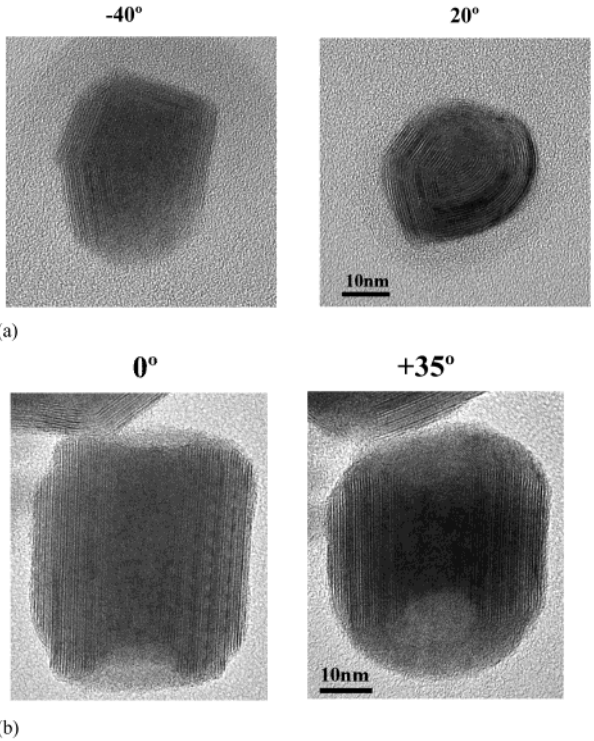


***Figure 3.*** TEM images of (a) nested polyhedron and (b) short nanotube, observed at various tilt angles. Note that for clarity a few tilt angles were omitted.

mean either that the structure was not completely closed[2] or, as in the case of $CdCl_2$, that the closed polyhedra are highly faceted. Also, the shape of the $SnS_2$ polyhedra is very irregular, which can be easily verified by looking at a tilted sample (Figure 3). The corner with right angle (90°) inclination (Figure 2b) is indicative of the existence of a square (rhombi) point defect in the corner of the faceted nanoparticle.[3,4] It was previously suggested that disposing such six rhombi symmetrically may lead to the formation of nano-octahedra,[4,14] which can be envisaged as the analogue of $C_{60}$ in $MoS_2$ ($SnS_2$), i.e., the most stable fullerenic structure.

After sonication of the soot in ethanol solution, as-prepared $SnS_2$ nanoparticles had a tendency to self-assemble into a two-dimensional pattern. This phenomenon is attributed to the attractive van der Waals forces between the nanoparticles,[15] as shown in Figure 4. This tendency was particularly emphasized

(13) Popovitz-Biro, R.; Twersky, A.; Rosenfeld Hacohen, Y.; Tenne, R. *Isr. J. Chem.* **2001**, *41*, 7.

(14) Tenne, R. *Adv. Mater.* **1995**, *7*, 965.
(15) Ge, G.; Brus, L. *J. Phys. Chem. B* **2000**, *104*, 9573.

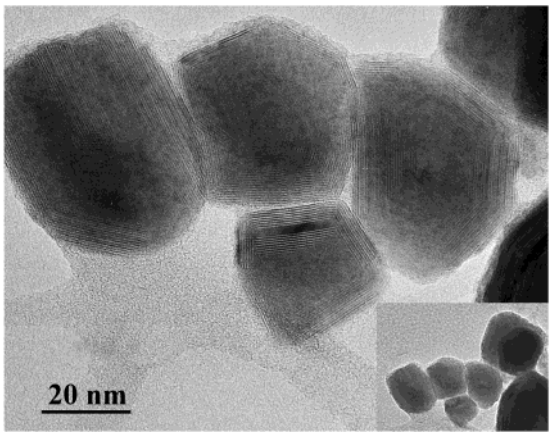


***Figure 4.*** TEM image of self-assembled $SnS_2$ nanoparticles obtained by sonication of the laser-ablated soot. Inset: overview of the same group of nanoparticles.

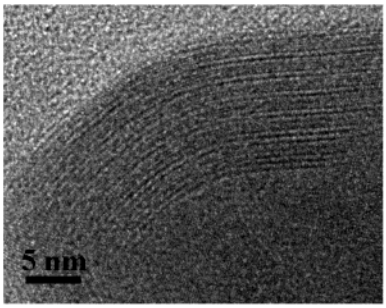


***Figure 5.*** HRTEM image of a part of a $SnS_2$ polyhedron.

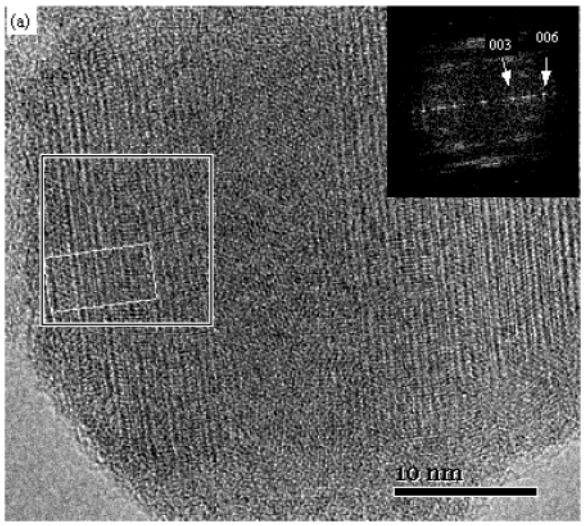


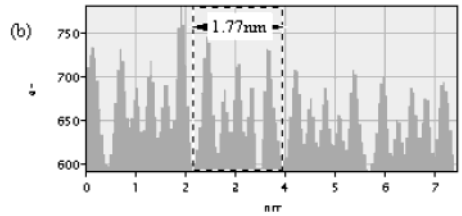


***Figure 6.*** (a) HRTEM micrograph of a short tubular nanoparticle showing superstructure lattice pattern. FFT of the area enclosed in the square is shown in the inset. (b) Line profile of a superstructure, integrated along the region enclosed in the rectangle.

by faceted nanoparticles, which were adjoined in the corners. Due to the polydispersity of the nanocrystallites' sizes (10−100 nm) and shapes, this ordering is of a short-range nature, only.

EDS analysis of the amorphous nanodots and the various round and polyhedral particles revealed that the S:Sn atomic ratio $x$:1 of the soot was variable ($x = 1.3-1.6$). The S:Sn ratio for bulk $SnS_2$ and SnS platelets was found to be 2.2 and 0.8, respectively. It is not unlikely that some sulfur loss was induced by tin disulfide decomposition in the hot plasma zone, induced by the laser beam ablation.

Some of the polyhedral and tubular structures consist of layers showing periodic or almost periodic patterns (superstructure), whereas others exhibited evenly spaced fringes. Figure 5 shows a magnified image of a part of a polyhedron with a repeating pattern of weak fringes between two dark fringes. Bulk $SnS_2$ crystal, on the other hand, did not reveal any superstructure of that kind, nor were they observed in closed polyhedra of $SnS_2$ produced by reaction of $SnO_2$ nanoparticles with $H_2S$ in a reducing atmosphere.[16] Such superstructures have not been observed in fullerene-like structures of other transition metal dichalcogenides or other layered compounds.

Careful examination of some HRTEM images (Figure 6) of nanoparticles with superstructures reveals that the superlattice consists of a periodic stacking of two types of layers, which can be interpreted as $SnS_2$ and SnS layers. As mentioned above, the $SnS_2$ has a three-atom layered structure with the Sn atom layer sandwiched between two layers of sulfur. The layers are stacked together by weak van der Waals forces and have a large van der Waals (vdW) gap between them. This strucrture results in a high contrast, when viewed in an edge-on orientation. On the contrary, SnS has a two-atom layered structure containing both types of atoms in each layer, thus creating a double layer with similar densities in both layers. Computer simulation of the HRTEM images (MacTempas) viewed along the layers of the two structures gives further support for the current interpretation of the contrast. Fast Fourier transform (FFT) of this ordered pattern, enclosed in the square frame, is shown in the inset. Fourier filtering of the 00$l$ reflections further extenuates the periodicity of the superstructure fringes. The line-profile of such ordered superlattice regions, enclosed in the rectangular frame, clearly shows the difference between these two types of layers (Figure 6b). In certain faceted particles the observed stacking is believed to consist of two SnS (O-orthorhombic) and one $SnS_2$ (T-trigonal) layer in the order O,O,T,O,O,T, .... The periodicity of this superstructure is ∼1.77 nm. In other nanoparticles of quasi spherical shape the stacking order is O,T,O,T, ... with a periodicity of ∼1.18 nm. These ordered regions are rather limited to small areas. The interlayer distance of bulk $SnS_2$ is 0.5899 nm, and that of bulk SnS is 0.56 nm. Using the bulk layer spacing of each structure, the calculated periodicity for the superstructure of type O,O,T,O,O,T, ... is 1.71 nm and that of the superstructure of the type O,T,O,T, ... is 1.15 nm. On the average, therefore, there is a net expansion of 2.6% along the layer spacing axis if one considers a superstructure of the type O,T,O,T, ... and an expansion of 3.5% for a O,O,T,O,O,T, ... superstructure. Lattice expansion along the $c$-axis was previously observed in nested carbon fullerenes and carbon nanotubes as well as in other *IF* nanostructures and

(16) Alperson, B.; Homyonfer, M.; Tenne, R. *J. Electroanal. Chem.* **1999**, *473*, 186.

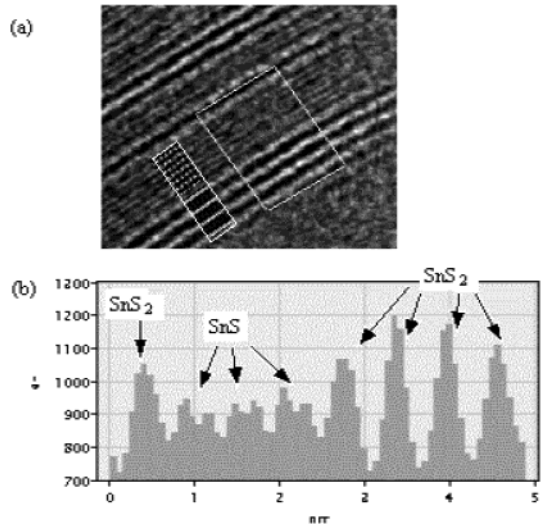


***Figure 7.*** (a) HRTEM micrograph and (b) line profile (from the area enclosed in the large rectangle), showing stacking disorder of the SnS and $SnS_2$ layers. The small rectangle in the image (a) shows an overlay of the simulated O−O−O−T−T−T−T stacking. The simulation parameters used are 5 nm thickness and −40 nm defocus.

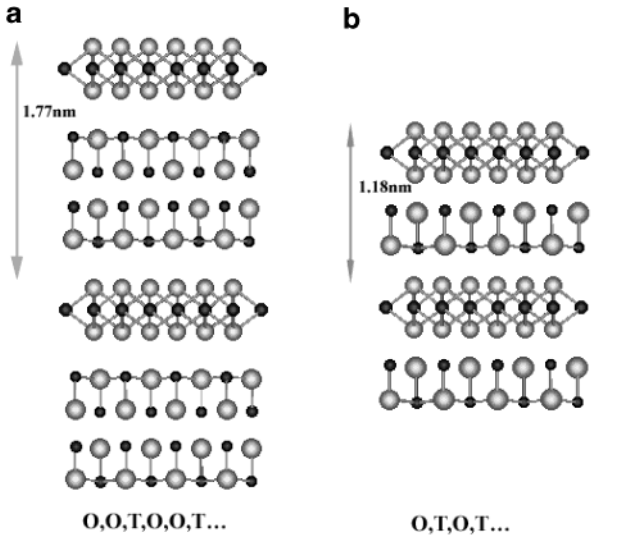


***Figure 8.*** Illustration of the two mainly observed superstructures: O,O,T,O,O,T, ... (a) and O,T,O,T, ... (b).

is believed to be responsible for the strain relief mechanism in folded nanostructures.[17,18] Some nanoparticles show stacking disorder as shown in Figure 7. Further support for the stacking disorder of the two lattices was obtained from the line profile (Figure 7b) and the simulation of the HRTEM image (see small rectangle in Figure 7a). Such disorder explains the fact that the only 00*l* reflections observed when taking the ED pattern from the entire particle or from several particles together is the basic spacing of 0.59 nm between the stacked layers. These results are consistent with the X-ray powder diffraction data, which shows a single 00*l* line with a 0.59 nm spacing, and the Raman spectra of the nanopowder, which is typical of bulk $SnS_2$.

Further EDS analyses were performed on single polyhedral nanoparticles. The obtained S:Sn ratio varied between 1.2 and 1.4, strongly indicating the existence of a mixture of the above two phases in the nanostructure. More specifically, a 1:1 (SnS/$SnS_2$)—O,T,O,T, ...—superstructure or a 2:1 (SnS/$SnS_2$)—O,O,T,O,O,T, ...—superstructure would be expected to result in a S:Sn atomic ratio of 1.5 or 1.33, respectively.

Tubular morphologies exist in misfit compounds of the type $(AX)_{1+y}(BX_2)_n$.[19,20] Here $BX_2$ is a metal dichalcogenide compound with a layered structure and AX is another metal chalcogenide having a cubic structure. The tubular morphology is a result of the lattice mismatch between the two sublattices comprising the host−guest structure (for a review see ref 21). The superstructures observed in the present study can be considered as a new kind of misfit structure, where both constituents crystallize in a layered structure and have a common metal atom with two different valences. Figure 8 illustrates the two mainly observed superstructures: O,O,T,O,O,T, ... (a) and O,T,O,T, ... (b). The sulfur volatility during the ablation process induces the crystallization of several types of sulfur-deficient misfit structures. The superstructure of the type O,O,T,O,O,T, ... is more abundant for the faceted and tubular topologies (Figure 2b), whereas that of the type O,T,O,T, ... is more often observed in the quasi spherical morphologies. These superstructures are stabilized by a partial charge transfer from the Sn(II) of the SnS (guest) sublattice to Sn(IV) of the $SnS_2$ (host layer).[22] One may therefore consider the misfit between two lattices as a new stimulus for the folding of the layers, resulting in *IF* structures. This driving force comes on top of the already established closure mechanism, i.e., annihilation of dangling bonds at the periphery of the layers of the *IF* nanostructures. Alternatively, one may envisage the annihilation of dangling bonds in misfit compounds as an additional factor leading to their tubular structure.

Both $SnS_2$ and SnS melt congruently at 865 and 880 °C, respectively. Thus, in addition to the plume of the ablated target, sulfur-deficient nanodropletes of the ablated target are ejected from the surface. Such droplets quench very rapidly to ambient temperature and may form amorphous nanodots. Alternatively, some of the amorphous nanodots could crystallize during cooling to form the spherical nanoparticles with superlattice structure. This mechanism is a possible explanation for the formation of the spherical fullerene-like nanoparticles.

## 5. Conclusions

Laser ablation of $SnS_2$ powder resulted in nanoparticles of polyhedral and short tubular forms with sulfur deficiency. Some of the nanoparticles showed periodic or semiperiodic superstructure, as evidenced from TEM and HRTEM images. Analysis of the nanoparticle structures suggests that they can be viewed as a misfit layer structure of $SnS_2$ and SnS in different periodicities. Accordingly, an additional mechanism for the closure of *IF* nanostructures is proposed. Furthermore, it suggests that the annihilation of dangling bonds at the rim is

(17) Feldman, Y.; Wasserman, E.; Srolovitz, D. J.; Tenne, R. *Science* **1995**, *267*, 222.
(18) Feldman, Y.; Frey, G. L.; Homyonfer, M.; Lyakhovitskaya, V.; Margulis, L.; Cohen, H.; Hodes, G.; Hutchison, J. L.; Tenne, R. *J. Am. Chem. Soc.* **1996**, *118*, 5362.
(19) Gomez-Herrero, A.; Landa-Canovas, A. R.; Hansen, S.; Otero-Diaz, L. C. *Micron* **2000**, *31*, 587.
(20) Bernaerts, D.; Amelinckx, S.; Van Tendeloo, G.; Van Landuyt, J. *J. Cryst. Growth* **1997**, *172*, 433.
(21) Rouxel, J.; Meerschaut, A.; Weigers, G. A. *J. Alloys Comp.* **1995**, *229*, 144.
(22) Cario, L.; Palvadeau, P.; Lafond, A.; Deudon, C.; Moelo, Y.; Corraze B.; Meerschaut, A. *Chem. Mater.* **2003**, *15*, 943.

another factor leading to the formation of tubules in misfit compounds.

**Acknowledgment.** We are grateful to Dr. Y. Feldman for the assistance with some of the analyses reported in this work. The mechanism of congruent melting and subsequent crystallization of the nanoparticles was proposed by one of the reviewers. This work was supported by a grant from the Israeli Ministry of Science. S.Y.H. is grateful to the Israeli Ministry of Foreign Affairs for a Fellowship.

JA036057D